AIP | The Journal of Chemical Physics

Photoelectron spectroscopic and theoretical study of the [HPd(η2-H2)]− cluster anion

Xinxing Zhang, Paul J. Robinson, Gerd Ganteför, Anastassia Alexandrova, and Kit H. Bowen

Citation: The Journal of Chemical Physics **143**, 094307 (2015); doi: 10.1063/1.4929998
View online: http://dx.doi.org/10.1063/1.4929998
View Table of Contents: http://scitation.aip.org/content/aip/journal/jcp/143/9?ver=pdfcov
Published by the AIP Publishing

Photoelectron spectroscopic and theoretical study of the $[HPd(\eta^2\text{-}H_2)]^-$ cluster anion

Xinxing Zhang (张新星),[1] Paul J. Robinson,[2] Gerd Ganteför,[1]
Anastassia Alexandrova,[2,3,a)] and Kit H. Bowen[1,a)]
[1]*Departments of Chemistry and Materials Science, Johns Hopkins University, Baltimore, Maryland 21218, USA*
[2]*Departments of Chemistry and Biochemistry, University of California, Los Angeles, Los Angeles, California 90095-1569, USA*
[3]*California NanoSystems Institute, 570 Westwood Plaza, Building 114, Los Angeles, California 90095, USA*

(Received 31 July 2015; accepted 21 August 2015; published online 4 September 2015)

Anion photoelectron spectroscopic and theoretical studies were conducted for the PdH^- and PdH_3^- cluster anions. Experimentally observed electron affinities and vertical detachment energies agree well with theoretical predictions. The PdH_3^- anionic complex is made up of a PdH^- sub-anion ligated by a H_2 molecule, in which the H–H bond is lengthened compared to free H_2. Detailed molecular orbital analysis of PdH^-, H_2, and PdH_3^- reveals that back donation from a *d*-type orbital of PdH^- to the σ* orbital of H_2 causes the H–H elongation, and hence, its activation. The H_2 binding energy to PdH^- is calculated to be 89.2 kJ/mol, which is even higher than that between CO and Pd. The unusually high binding energy as well as the H–H bond activation may have practical applications, e.g., hydrogen storage and catalysis. © *2015 AIP Publishing LLC.* [http://dx.doi.org/10.1063/1.4929998]

INTRODUCTION

The interaction between transition metals (TM) and hydrogen has always been an intriguing research topic, with applications in hydrogen storage[1–3] and the catalysis[4,5] of hydrogenation and dehydrogenation reactions. Special bonding motifs between transition metal atoms and hydrogen, beyond simple M–H σ bonds, are interesting not only because they are rarely reported but also because they could further our understanding of the nature of chemical bonding. Recently, our joint experimental/theoretical team discovered the $PtZnH_5^-$ cluster anion; it possessed an unprecedented planar pentagonal coordination between the H_5^- ring and Pt moieties and also exhibited special σ-aromatic character.[6] In this species, the H_5^- ring moiety as a whole can be viewed as a η^5-H_5 ligand interacting with Pt, and it is in turn stabilized by the Pt atom.

In 1991, using IR spectroscopy and theoretical calculations, Schnöckel discovered a $[Cu(\eta^2\text{-}H_2)Cl]$ cluster in which a H_2 molecule was ligated to Cu. The H–H bond of the H_2 ligand was slightly elongated comparing to a free H_2 molecule.[7] More recently, Novick performed a study of $[Cu(\eta^2\text{-}H_2)F]$ and $[Ag(\eta^2\text{-}H_2)Cl]$ neutral clusters via microwave spectroscopy.[8,9] He found back-donation from a *d*-type orbital on these transition metals to the unoccupied σ* orbitals of H_2, this causing the elongation of the H–H bond. The occupied σ orbital of H_2 acts as a "lone pair" and inserts into the lowest unoccupied molecular orbital (LUMO) of the metal halide. In all of these cases, while the geometry of the H_2 moiety does not deviate much from that of the free H_2, the binding energies of H_2 to their transition metals (80–110 kJ/mol) are much greater than typical van der Waals interaction energies. Other η^2-H_2 ligation examples were discovered in more complicated transition metal complexes, such as those protected by N, P, or O-based ligands or the π-acceptor ligand, CO.[3,10–14]

In the present paper, we report an anion photoelectron spectroscopic (PES) study of the PdH_3^- cluster anion in which a H_2 molecule acts as a ligand to PdH^-. *Ab initio* calculations closely reproduce the experimental data, confirming the structure of the anion seen in the experiment. In order to understand the bonding between H_2 and PdH^-, the photoelectron spectrum of PdH^- as well as a molecular orbital (MO) analysis of PdH^-, PdH_3^-, and H_2 is also presented. The H–H bond in PdH_3^- is lengthened compared to that in the free H_2 molecule due to back donation from a *d*-type orbital of PdH^- to the LUMO (the σ* orbital) of H_2. The additional interactions of H_2 and PdH^- come from the bonding and anti-bonding combinations of the highest occupied molecular orbital (HOMO, the σ orbital) of H_2 and the σ bonding orbital of PdH^-.

EXPERIMENTAL AND THEORETICAL METHODS

This work utilized anion PES as its primary probe. Anion PES is conducted by crossing a mass-selected beam of negative ions with a fixed-energy photon beam and energy analyzing the resulting photodetached electrons. This technique is governed by the energy conservation relationship, hν = EBE + EKE, where hν, EBE, and EKE are the photon energy, electron binding (transition) energy, and the electron kinetic energy, respectively. Our photoelectron spectrometer, which has been described previously, consists of one of the several ion sources, a linear time-of-flight mass spectrometer, a mass gate, a momentum decelerator, a neodymium-doped yttrium aluminum garnet (Nd:YAG) laser for photodetachment, and a magnetic bottle electron energy analyzer having a resolution of 35 meV at EKE = 1 eV.[15]

a)Electronic addresses: kbowen@jhu.edu and ana@chem.ucla.edu

Photoelectron spectra were calibrated against the well-known photoelectron spectrum of Cu^-.[16] $PdH_{1,3}^-$ anions were generated using a pulsed arc cluster ionization source (PACIS), which has been described elsewhere.[17] A ~30 μs duration, 180 V electrical pulse applied across the anode and sample cathode of the discharging chamber vaporized the Pd atoms. The sample cathode was prepared by firmly pressing Pd powder onto a copper rod. Almost simultaneously, 200 psi of ultra-high purity hydrogen gas was injected into the discharge region, where it was dissociated into hydrogen atoms. The resulting mixture of atoms, ions, and electrons then reacted and cooled as it flowed along a 15 cm tube before exiting into high vacuum. The resulting anions were then extracted and mass-selected prior to photodetachment.

Density functional theory calculations were conducted by applying PBEPBE functional[18] using the Gaussian09 software package[19] to determine the geometries of the anionic and neutral clusters. The 6-311++G (3df, 3pd) basis set[20] on H and the Stuttgart Dresden (SDD) basis set[21] on Pd were used. The PdH, PdH^-, PdH_3, and PdH_3^- clusters were all initially treated with ROHF SCF with the aug-CC-pVTZ-PP[22] basis set on the Pd atom, and the ATZP[23] basis set on H atoms. The wavefunctions were then read in the CCSD(T)[24] and equation of motion coupled-cluster singles doubles and perturbative triples (EOM-CCSD(T))[25] calculations. The adiabatic detachment energy (ADE) is the energy difference between the anion and the neutral relaxed to the anion's nearest local minimum. If the local minimum is also the global minimum, the ADE is also the adiabatic electron affinity (EA). The vertical detachment energy (VDE) was obtained by subtracting the energy of the neutral cluster calculated at the geometry of the anion from the energy of the anion. Deeper transitions were calculated by adding the electronic excitation energies of the neutral to the VDE. We note that the agreement with the experimental spectrum improved dramatically with the increase of the basis sets, and also the inclusion of the perturbative-triple excitations in CCSD(T) (EOM-CCSD was insufficient). All calculations were carried out using NW Chem software[26] and all visualizations of orbitals were generated with VMD.[27] Atomic charges were calculated using Natural Population Analysis (NPA)[28] in Gaussian 09 with the SDD basis set on Pd and TZVP[29] basis set on H. The NPA method has been found to be satisfactory in calculating the charge distribution within a cluster.[30,31] Density functional theory was implemented using the B3LYP[32] hybrid functional.

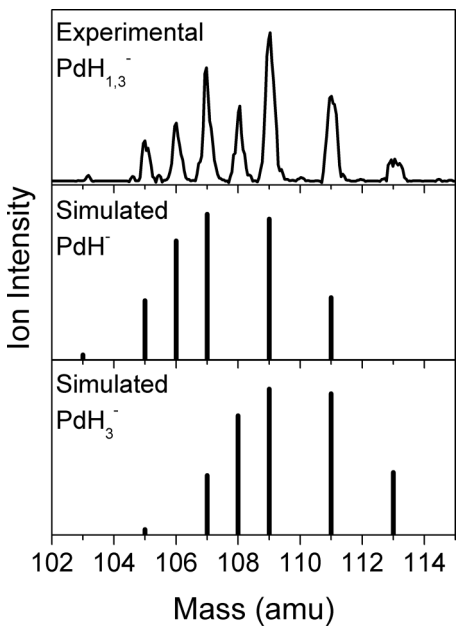

FIG. 1. The mass spectrum showing $PdH_{1,3}^-$ and the simulated isotopic distributions for both PdH^- and PdH_3^-.

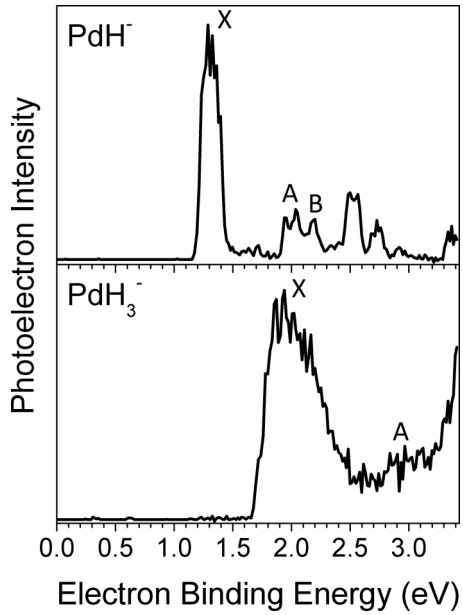

FIG. 2. The anion photoelectron spectra of PdH^- and PdH_3^-, each taken with 3.49 eV laser.

RESULTS AND DISCUSSION

Figure 1 presents a portion of the mass spectrum, showing the $PdH_{1,3}^-$ anions. Due to isotopic congestion from Pd and from two different Pd/H stoichiometries, the mass spectrum

TABLE I. Our anion photoelectron spectral transitions compared to those from my calculations (in eV). Peak X denotes the vertical detachment energy (VDE). Peaks A and B denote photodetachment from deeper MOs. The final electron configurations after photodetachment are also presented.

Species	Expt.	Theoretical[a]	Final configuration
PdH^-	EA ~ 1.2	ADE 1.288	N/A
	X 1.29	1.29	$\ldots 1\Sigma+^2, \Pi^4, \Delta^4, 2\Sigma^1$
	A 2.04	2.07[b]	$\ldots 1\Sigma+^2, \Pi^4, \Delta^3, 2\Sigma^2$
	B 2.22	2.39[b]	$\ldots 1\Sigma+^2, \Pi^3, \Delta^4, 2\Sigma^2$
PdH_3^-	EA ~ 1.7	ADE 1.784	N/A
	X 1.94	1.97	$\ldots 2a_1^2 2b_2^2 1a_2^2 3a_1^2 4a_1^1$
	A ~ 2.9	2.81	$\ldots 2a_1^2 2b_2^2 1a_2^2 3a_1^1 4a_1^2$
		2.81	$\ldots 2a_1^2 2b_2^2 1a_2^1 3a_1^2 4a_1^2$
		2.82	$\ldots 2a_1^2 2b_2^1 1a_2^2 3a_1^2 4a_1^2$
		3.19	$\ldots 2a_1^1 2b_2^2 1a_2^2 3a_1^2 4a_1^2$

[a]aug-CC-pVTZ-PP[23] basis set was used for Pd and ATZP basis set was used for H.
[b]Indicates doubly degenerate features.

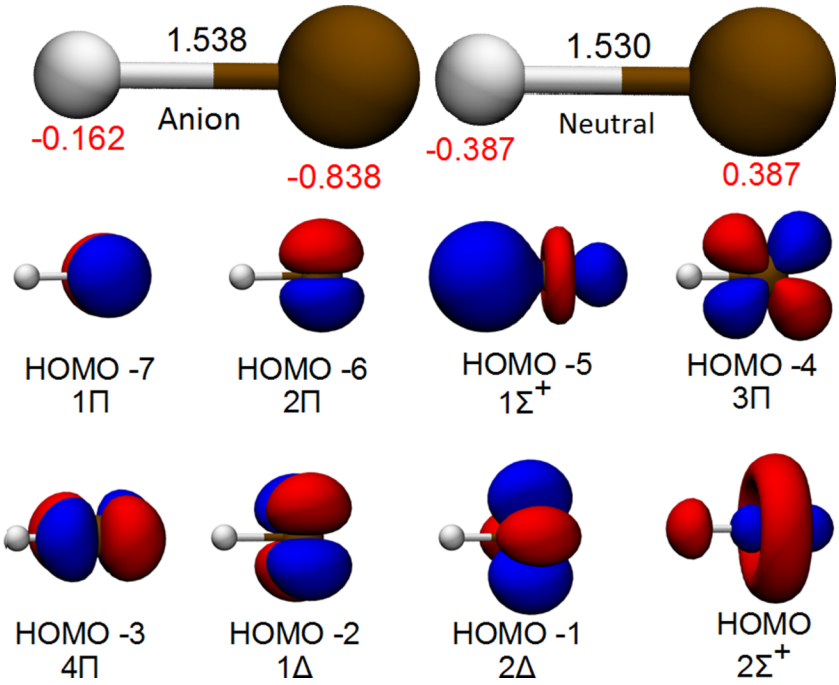

FIG. 3. The structures and MOs of $PdH^{-/0}$. Bond lengths (Å, in black) and NPA charge distributions (e, in red) are also included.

is complicated. To help dissect it, we have also presented simulated isotopic distributions for PdH^- and PdH_3^- below the actual mass spectrum. The very little ion intensity at mass = 110 indicates that there is only negligible Pd^- or PdH_2^- in the ion beam, which will not affect the PES. $PdH_{1,3}^-$ species are the major anions seen. The photoelectron spectrum of PdH^- was taken at mass = 106, and the photoelectron spectrum of PdH_3^- was taken at mass = 108 and 113. The lack of other PdH_n^- species in the mass spectrum suggests the special stabilities of $PdH_{1,3}^-$. Figure 2 presents the photoelectron spectra of PdH_1^- and PdH_3^-. For PdH^-, several peaks were observed. The positions of the first three peaks are marked by X, A, and B and are tabulated in Table I for comparison with the calculated spectra. The X peak located at 1.29 eV corresponds to the VDE. The A peak appears to show splitting, which may be due to the double degeneracy of this feature, as shown theoretically (see Figure 3). The peaks of PdH^- are relatively sharp, consistent with the fact that the structural difference between the anion and its neutral is small (see Figure 3). This leads to a large Franck-Condon overlap for this (origin) transition. The adiabatic EA, defined as the energy difference of the ground state of the anion and the ground state of the neutral, is estimated from the threshold of the first EBE band. The EA of PdH is thus estimated to be ~1.2 eV. The calculated ADE value is 1.288 eV (see Table I), in good agreement with the experimental value. Therefore, ADE and EA are actually one and same value in this case.

For PdH_3^-, the threshold EBE of a prominent broad band, X, occurs at ~1.7 eV (EA) and peaks at 1.94 eV (VDE). Other features can be observed on the higher EBE end, but

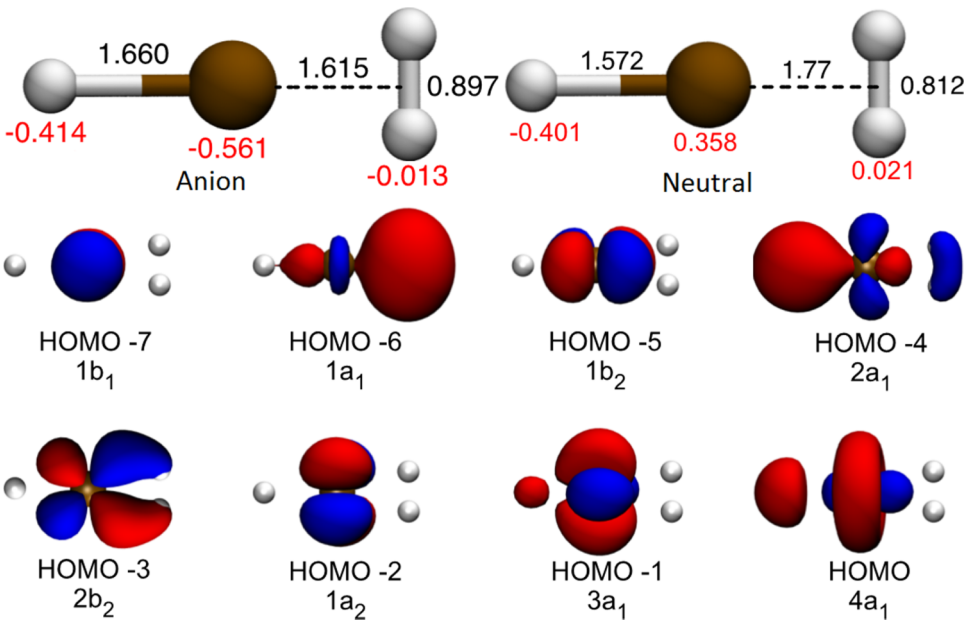

FIG. 4. The structures and MOs of $PdH_3^{-/0}$. Bond lengths (Å, in black) and NPA charge distributions (e, in red) are also included.

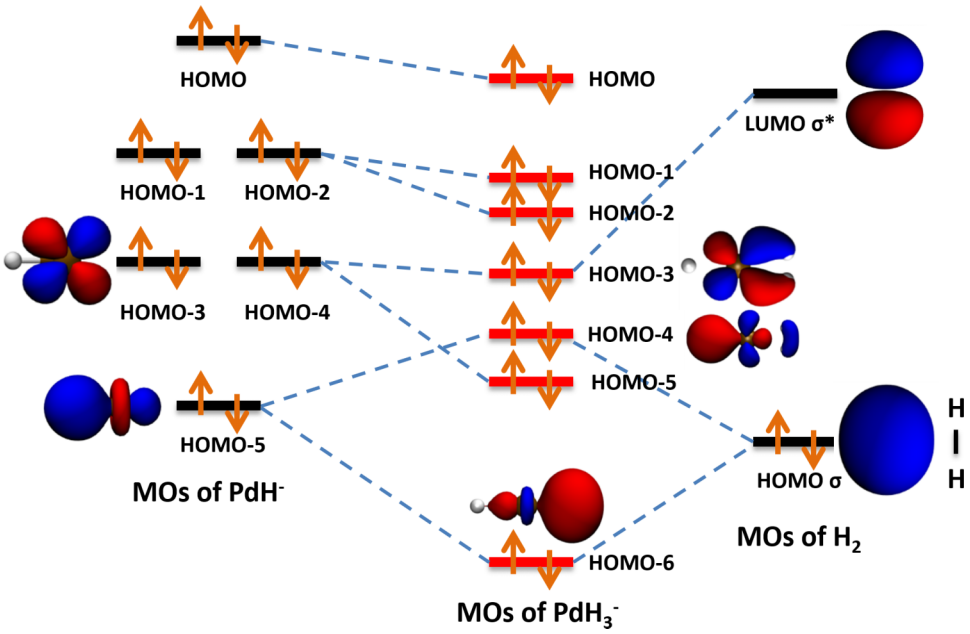

FIG. 5. The correlation diagram for the valence MOs of PdH_3^-.

they are not well-resolved. We tentatively indicate a peak at EBE = 2.9 eV, marked as A, but there could be more than one transition under these features, as indeed is supported by calculations. The relatively broad peak in the PdH_3^- spectrum suggests significantly more structural difference between the anion and its neutral than was seen in the case of PdH^- and its corresponding neutral. The calculated ADE value is 1.784 eV; this value agrees well with experiment. Again, ADE and EA are the same. Excellent agreements between experimental and theoretical values can be observed in Table I. The final electron configurations corresponding to each photodetachment transition are also displayed in Table I, and the MOs from which the corresponding electron detachments take place are depicted in Figures 3 and 4.

The calculated results for $PdH^{-/0}$ and $PdH_3^{-/0}$, including bond lengths (Å, in black), NPA charge distributions (*e*, in red), and molecular orbitals (MO) are displayed in Figures 3 and 4. For PdH^-, the Pd–H bond distance is 1.538 Å, very close to that of the neutral (1.530 Å). The Pd atom takes most of the negative charge. The HOMO-5 and HOMO are the bonding and anti-bonding orbitals of the Pd–H single bond from the combination of d_z^2 orbital of Pd and *s* orbital of H. The HOMO-1 to HOMO-4 are the non-bonding *d* orbitals of Pd, and the HOMO-6, HOMO-7 are the non-bonding *p* orbitals of Pd.

For PdH_3^-, the Pd–H bond length is 1.660 Å, slightly longer than that of PdH^-, and the H–H moiety clearly shows a η^2 type of ligation. At this stage, we can formally write PdH_3^- as $[HPd(\eta^2\text{-}H_2)]^-$ as it appears in the title. The H–H bond length is 0.897 Å, 20% longer than free H_2 molecule (0.747 Å), indicating that the H–H bond is activated. The NPA charge distribution shows that the H–H moiety is partially negatively charged, which is consistent with the bond elongation and back-donation from the Pd atom. In neutral PdH_3, the H_2 molecule is further away from the PdH moiety and the H–H bond length is closer to free H_2, indicating a weaker interaction between H_2 and PdH. The charge on Pd is positive, and thus, the back donation from Pd to H_2 is smaller, causing the positive charge on H_2 moiety. Figure 5 is the correlation diagram depicting how the MOs of $[HPd(\eta^2\text{-}H_2)]^-$ are formed from the combinations of the MOs of PdH^- and H_2. The HOMO-4, which is a *d*-type orbital of PdH^-, back donates into the LUMO of H_2 and forms the HOMO-3 of $[HPd(\eta^2\text{-}H_2)]^-$. This is the combination that causes the H–H bond elongation, charge transfer to H_2, and its activation. HOMO-5 of PdH^- combines with the HOMO of H_2 and splits into HOMO-4 and HOMO-6 of PdH_3^-. HOMO-4 represents the anti-bonding orbital between H_2 and PdH^-, and HOMO-6 is the bonding orbital. HOMO, HOMO-1, HOMO-2, and HOMO-5 of PdH_3^- are non-bonding orbitals belonging only to PdH^-, which are displayed in Figure 4. Note that the degenerate HOMO-1 and HOMO-2 of PdH^- lose degeneracy in PdH_3^- due to symmetry breaking.

The binding energy, D_0, of the η^2-H_2 moiety to the PdH^- sub-ion is calculated from the following formula with the CCSD(T) level of theory: $D_0 = E(PdH^-) + E(H_2) - E(PdH_3^-) = 89.2$ kJ/mol. This number is comparable to the binding energies between H_2 and transition metal halides[7–9] and higher than the binding energy between Pd and the much more commonly used ligand, CO.[33,34]

CONCLUDING REMARKS

Since Pd^- is isovalent to Cu and isoelectronic to Ag, it is not surprising that H_2 also binds to them.[7–9] Nevertheless, there are also significant differences. For example, since the electron-withdrawing halide atoms in CuCl, CuF, and AgCl reduce the electron density on their transition metal atoms, the extent of H_2 back donation in those cases, e.g., CuCl–H_2, is also reduced compared to that in PdH_3^-. More generally, while the H_2 moieties in PdH_3^- are negatively charged, there are many other examples where H_2 ligands are positively charged.[3] Still, negatively charged hydrogen is key to some processes, e.g., the hydrogenation of CO_2.[35]

The H_2 bond length in the present study is calculated to be 20.0% longer than in the free H_2 molecule and around 12.5% longer than those reported for H_2 adducts with CuCl, CuF, and AgCl.[7–9] This shows that the H–H bond is more activated in PdH_3^-. The H–H bond length and charge distribution differences between PdH_3^- and PdH_3 are also examples of the extent of back-donation. In neutral PdH_3, for example, the H_2 moiety is less activated than in anionic PdH_3^-, although it is similarly activated compared to H_2 adducts with CuCl, CuF, and AgCl.[7–9] Thus, PdH_3^- might have a role in catalysis. Also, when palladium is used as hydrogen storage material, the best stoichiometry that has been achieved is $PdH_{0.6}$, with a hydrogen mass density of 0.56%.[1] If one were to view the H_2 ligand in PdH_3^- as the stored hydrogen, then the hydrogen mass density would be 1.86%. Thus, if PdH_3^- could exist in a bulk material, it might have attributes as a hydrogen storage material.

ACKNOWLEDGMENTS

We thank Stewart Novick for discussions and insightful comments. This material is based upon work supported by the Air Force Office of Scientific Research (AFOSR) under Grant No. FA9550-15-1-0259 (K.H.B.) and BRI Grant No. FA9550-12-1-0481 (A.N.A.). P.J.R. received support from Sigma Xi Grants-in-Aid for Research, the UCLA Department of Chemistry and Biochemistry, the UCLA College Honors Program, and the UCLA Undergraduate Research Center-Sciences. Computational resources were provided by the UCLA-IDRE Cluster.

[1]L. Schlapbach and A. Züttel, Nature **414**, 353 (2001).
[2]W. Grochala and P. P. Edwards, Chem. Rev. **104**, 1283 (2004).
[3]G. J. Kubas, Chem. Rev. **107**, 4152 (2007).
[4]J. A. Widegren and R. G. Finke, J. Mol. Catal. A **191**, 187 (2003).
[5]G. E. Dobereiner and R. H. Crabtree, Chem. Rev. **110**, 681 (2010).
[6]X. Zhang, G. Liu, G. Gantefoer, K. H. Bowen, and A. N. Alexandrova, J. Phys. Chem. Lett. **5**, 1596 (2014).
[7]H. S. Plitt, M. R. Bär, R. Ahlrichs, and H. Schnöckel, Angew. Chem., Int. Ed. Engl. **30**, 832 (1991).
[8]G. S. Grubbs II, D. A. Obenchain, H. M. Pickett, and S. E. Novick, J. Chem. Phys. **141**, 114306 (2014).
[9]D. J. Frohman, G. S. Grubbs II, Z. Yu, and S. E. Novick, Inorg. Chem. **52**, 816 (2013).
[10]B. Chaudret, G. Chung, O. Eisenstein, S. A. Jackson, F. J. Lahoz, and J. A. Lopez, J. Am. Chem. Soc. **113**, 2315 (1991).
[11]M. L. Christ, S. Sabo-Etienne, and B. Chaudret, Organometallics **13**, 3800 (1994).
[12]G. J. Kubas, R. R. Ryan, B. I. Swanson, P. J. Vergamini, and H. J. Wasserman, J. Am. Chem. Soc. **106**, 452 (1984).
[13]N. Aebischer, U. Frey, and A. E. Merbach, Chem. Commun. **1998**, 2303.
[14]S. L. Matthews, V. Pons, and D. M. Heinekey, J. Am. Chem. Soc. **127**, 850 (2005).
[15]M. Gerhards, O. C. Thomas, J. M. Nilles, W. J. Zheng, and K. H. Bowen, J. Chem. Phys. **116**, 10247 (2002).
[16]J. Ho, K. M. Ervin, and W. C. Lineberger, J. Chem. Phys. **93**, 6987 (1990).
[17]X. Zhang, Y. Wang, H. Wang, A. Lim, G. Ganteför, K. H. Bowen, J. U. Reveles, and S. N. Khanna, J. Am. Chem. Soc. **135**, 4856 (2013).
[18]J. P. Perdew, K. Burke, and M. Ernzerhof, Phys. Rev. Lett. **77**, 3865 (1996).
[19]M. J. Frisch, G. W. Trucks, H. B. Schlegel, G. E. Scuseria, M. A. Robb, J. R. Cheeseman, G. Scalmani, V. Barone, B. Mennucci, G. A. Petersson *et al.*, GAUSSIAN 09, Revision A.1, Gaussian, Inc., Wallingford, CT, 2009.
[20]R. Krishnan, J. S. Binkley, R. Seeger, and J. A. Pople, J. Chem. Phys. **72**, 650 (1980).
[21]M. Dolg, H. Stoll, H. Preuss, and R. M. Pitzer, J. Phys. Chem. **97**, 5852 (1993).
[22]K. A. Peterson, D. Figgen, M. Dolg, and H. Stoll, J. Chem. Phys. **126**, 124101 (2007).
[23]P. A. Fantin, P. L. Barbieri, A. C. Neto, and F. E. Jorge, J. Mol. Struct. **810**, 103 (2007).
[24]K. Raghavachari, G. W. Trucks, J. A. Pople, and M. Head-Gordon, Chem. Phys. Lett. **157**, 479 (1989).
[25]J. D. Watts and R. J. Bartlett, Chem. Phys. Lett. **233**, 81 (1995).
[26]M. Valiev, E. J. Bylaska, N. Govind, K. Kowalski, T. P. Straatsma, H. J. J. van Dam, D. Wang, J. Nieplocha, E. Apra, T. L. Windus, and W. A. de Jong, Comput. Phys. Commun. **181**, 1477 (2010).
[27]W. Humphrey, A. Dalke, and K. J. Schulten, J. Mol. Graphics **14**, 33 (1996).
[28]A. E. Reed, R. B. Weinstock, and F. Weinhold, J. Chem. Phys. **83**, 735 (1985).
[29]N. Godbout, D. R. Salahub, J. Andzelm, and E. Wimmer, Can. J. Chem. **70**, 560 (1992).
[30]H. Wang, X. Zhang, J. Ko, A. Grubisic, X. Li, G. Ganteför, H. Schnöckel, B. Eichhorn, M. Lee, P. Jena, A. Kandalam, B. Kiran, and K. H. Bowen, J. Chem. Phys. **140**, 054301 (2014).
[31]H. Wang, Y. Ko, X. Zhang, G. Gantefoer, H. Schnoeckel, B. W. Eichhorn, P. Jena, B. Kiran, A. K. Kandalam, and K. H. Bowen, J. Chem. Phys. **140**, 124309 (2014).
[32]A. D. Becke, J. Chem. Phys. **98**, 5648 (1993).
[33]J. Li, G. Schreckenbach, and T. Ziegler, J. Am. Chem. Soc. **117**, 486 (1995).
[34]V. Jonas and W. Thiel, J. Chem. Phys. **102**, 8474 (1995).
[35]H. K. Gerardi, A. F. DeBlase, X. Su, K. D. Jordan, A. B. McCoy, and M. A. Johnson, J. Phys. Chem. Lett. **2**, 2437 (2011).